NAL PROPOSAL No. 49

Correspondent: J. A. Poirier
Physics Department
University of Notre Dame
Notre Dame, Ind. 46556

Phone: 219-283-6011

THE ELECTROMAGNETIC FORM FACTOR OF THE CHARGED PION FROM π^+e^- ELASTIC SCATTERING

N. N. Biswas, N. M. Cason, V. P. Kenney
J. A. Poirier, O. R. Sander, W. D. Shephard
University of Notre Dame

T. E. Toohig
National Accelerator Laboratory

June, 1970

NAL PROPOSAL

I. Cover Page.

1. Title of Experiment: The Electromagnetic Form Factor of the Charged Pion from π^+e^- Elastic Scattering

2. a. Experimenters: N. N. Biswas, N. M. Cason, V. P. Kenney, J. A. Poirier, O. R. Sander, W. D. Shephard plus one additional Ph.D., Physics Department, University of Notre Dame; T. E. Toohig, National Accelerator Laboratory.

   b. Graduate Students: Two graduate students.

   c. Engineer: W. L. Rickhoff

3. Summary:

We propose to study the reaction $\pi^+e^- \rightarrow \pi^+e^-$ at 100 GeV/c with a wire spark chamber spectrometer and on-line computer. The events of this reaction with the largest recoil electron energy (and therefore largest 4-momentum transfer squared, q^2) are of interest in determining the q^2-dependence of the electromagnetic form factor of the charged pion in the classic way. The largest q^2, .0855 $(GeV/c)^2$, gives an $|F_\pi|^2 = 0.77$. This high statistics, high precision experiment will be able to easily see this effect and study it as a function of q^2.

4. a. NAL Equipment Required for the Experiment:
   i. An 18 kg 3m-long magnet with an aperture in excess of 8 x 13 $in.^2$
   ii. Liquid hydrogen target, 2" dia. x ~20".
   iii. Miscellaneous items of electronics.
   iv. Beam Cerenkov counters.
   v. Small amounts of computer time including 6 one-minute high-priority runs per day during the scheduled run.

   b. Major Items of Equipment to be Furnished by the Collaboration:
   i. Charpak chambers and readout electronics.
   ii. Magnetostrictive chambers and readout electronics.
   iii. Varian Data 620i on-line computer and magnetic tape transport.
   iv. Some fast electronics.
   v. Electronics trailer.
   vi. Shower counters.
   vii. Misc. counters.

   Item (i) is to be furnished by the NAL part of the collaboration. Items (ii), (iii), (iv), (v) are to be furnished by the Notre Dame part of the collaboration; these items already exist.

   The responsibility for items (vi) and (vii) will be shared in an equitable way between the collaborators.

5. Beam Requirements

A π^+ beam of 80-100 GeV/c in the 2.5 mrad high resolution beam in Area 2 with an intensity of $\sim 10^6$/burst with a > 500 msec flattop.

6. Estimate of Running Time Required

Data	500 hours
Tests, empty target, calibration, etc.	500 hours
Total	1000 hours

7. Data Analysis

The experimental data from the magnetostrictive chambers and pulse height from counters are read into the 620 i computer. Check tests and simple fits are made and crude on-line results obtained with this computer. The raw data are written onto magnetic tape and analyzed off-line. To monitor the experiment a complete analysis of small samples of data will be done at NAL during the course of the experiment. The complete analysis of all the data will be done after the experiment and responsibility will be shared between the collaborators.

THE ELECTROMAGNETIC FORM FACTOR OF THE CHARGED PION FROM π^+e^- ELASTIC SCATTERING

N. N. Biswas, N. M. Cason, V. P. Kenney, J. A. Poirier,
O. R. Sander, W. D. Shephard, University of Notre Dame;
T. E. Toohig, National Accelerator Laboratory

II. Physics Justification

A. Introduction.

Extensive work has been invested in understanding the electromagnetic form factor, F_p, of the proton in the space-like region from electron-proton scattering experiments. The ρ, ω, and ϕ should contribute to this form factor but do not predict the observed q^{-8} fall-off of F_p^2 at high q^2. The electromagnetic form factor of the charged pion, F_π, should be determined by the ρ meson contribution; thus it should be much simpler to treat theoretically. Therefore a comparison of the results of the proposed experiment with theory might yield a significant clue to the electromagnetic structure of elementary particles.

Since the pion is an unstable particle with a lifetime of 26 nsec, it cannot be used as a target in the sense of the proton in e-p scattering. One can, however, use the inverse of the electron-nucleon scattering procedure to probe the pion structure. In this process beam pions are scattered off target electrons in a target. Crawford[1], in 1960, carried out such an experiment using 1.12 GeV/c π^- mesons incident on a hydrogen bubble chamber at Berkeley. An Aachen-Stockholm collaboration[2a] has done a similar experiment using 16 GeV/c π^- mesons in a CERN bubble chamber. Fitch and Leipuner[2b] have done a spark-chamber experiment at Brookhaven using 20 GeV/c π^- mesons to obtain higher

statistics for the process. Crawford[1] has pointed out that significant structural effects are not expected to begin to appear until the deBroglie wavelength of the target electron in the rest system of the bombarding pion is less than the Compton wavelength of the pion. This condition is satisfied for pion laboratory momenta ≥ 38 GeV/c.

The Born approximation is a simple approach to obtain an insight into the effect on electron scattering due to the size and radial shape of a charge distribution. The cross-section is proportional to the square of a form factor, $F(q^2)$, and is given by

$$\left(\frac{d\sigma}{dq^2}\right)_{\text{measured}} = F^2(q^2)\left(\frac{d\sigma}{dq^2}\right)_{\text{point charge}} \qquad (1)$$

where $q^2 = 2\, m_e\, T_e$; (1a)

q^2 is the square of the 4-momentum transfer to the scattered electron, m_e is the electron mass, and T_e is the kinetic energy of the scattered electron in the lab frame.

The pion form factor, $F_\pi(q^2)$, can be obtained by determining the ratio

$$F_\pi^2(q^2) = \left(\frac{d\sigma}{dT_e}\right)_{\text{meas}} \Big/ \left(\frac{d\sigma}{dT_e}\right)_{\text{point charge}}$$

for πe elastic scattering.

Rho dominance predicts the following behavior:

$$F_\pi = (1 + q^2/m_\rho^2)^{-1}$$

which would give $R_\pi = 0.63 \times 10^{-13}$ cm (see below).

B. Results of Previous Experiments.

Techniques other than elastic electron scattering have been

employed in the past to obtain F_π. The results for all of these methods can be characterized by a single parameter, the "radius" of the charge structure of the pion, R_π. This parameter is related to $F_\pi(q^2)$ by the relation $\langle R_\pi^2 \rangle = -6 \left. \frac{dF_\pi}{dq^2} \right|_{q^2 = 0}$.

Some results for R_π are given in Table I.

Table I. Techniques for Measuring the Pion Form Factor.

Experiment	Present Results	Method
π e elastic scattering[2]	$R_\pi < 3 \times 10^{-13}$ cm	direct experiment
$\pi^\pm$ a elastic scattering[3]	$R_\pi < 1 \times 10^{-13}$ cm	interference effect
$e^- p \rightarrow e^- n\pi^+$ scattering[4]	$R_\pi = (0.86 \pm 0.14) \times 10^{-13}$	isolation of a single diagram

The need for a direct measurement of R_π with good precision for values of R_π down to at least 0.6×10^{-13} cm is apparent.

C. Theoretical Cross Section and Radiative Corrections.

The elastic differential scattering cross section for a spin 0 particle scattering from an atom of Z point-charge electrons is given, to order α^2, by[5]

$$\left(\frac{d\sigma}{dT_e}\right)_{\substack{\text{pt.} \\ \text{chg.}}} = \frac{2\pi m_e r_e^2}{\beta^2} Z \frac{1}{T_e^2} \left(1 - \beta^2 \frac{T_e}{T_{max}}\right) \text{ cm}^2/\text{atom-GeV}$$

where m_e and r_e are the electron mass and its classical radius; T_e is the laboratory kinetic energy of the scattered electron; T_{max} is the maximum possible value of T_e for a given incident particle momentum, given by

$$2\,m_e\left(\frac{p^2}{m_e^2 + m^2 + 2\,m_e E}\right);$$

p, m, E, and β are the laboratory momentum, mass, total energy and velocity of the incident particle; and Z is the atomic number of the target material. (See Fig. 1)

The total cross-section, $\sigma(T_e \geq T_{min})$ where T_{min} is an arbitrary lower limit of T_e, is given by:

$$\sigma(T_e \geq T_{min}) = \frac{2\pi m_e r_e^2}{\beta^2} Z\left(\frac{1}{T_{min}} - \frac{1}{T_{max}} - \frac{\beta^2}{T_{max}} \ln\left(\frac{T_{max}}{T_{min}}\right)\right) \frac{cm^2}{atom} \quad (5)$$

For an extended pion the cross-section given by Eq. (4) is modified by the square of the form factor as shown in Eq. (1). The cross section must be further corrected to include terms of order α^3. These radiative corrections must be carefully calculated since some of the terms corresponding to real photon emission, depend intimately on the details of the experiment. Several different cases have been treated in the literature,[6] but none are directly applicable to the proposed experiment in which the energies and angles of the incoming pion and both the outgoing pion and electron are measured. Since the radiative corrections can be large and since the statistical and systematic uncertainties of the experiment will be kept as low as possibly (~ 1%), it will be necessary to do this calculation carefully.

D. Comparison with Other Planned Experiments

A similar experiment with a π^- beam has been proposed at lower energies at Serpukhov. At present, we have limited knowledge of the fine details of the experimental setup of this proposal. Thus a detailed comparison is not possible. However, the maximum available q^2 in their experiment is one-half or less than that of the present proposal. We also note that our use of a π^+ beam separates the final state π^+ and e^- particles in a magnetic field. This removes kinematic ambiguities and allows us to identify the characteristic electron shower in an easy manner. We also feel that the experiment should be repeated at NAL irrespective of the results of the proposed Serpukhov experiment due to the importance of the physics.

E. Conclusions

It will be possible at NAL to explore the structure of the pion down to distances of the order of 1/4 of the Compton wavelength of the pion. This corresponds to a maximum four-momentum transfer of 0.0857 $(GeV/c)^2$. The experiment can be done with high statistics and with precision on the order of 1% using presently known techniques. In the region of four-momentum transfer which is accessible, a deviation of as much as 24% from the point-charge $|F_\pi|^2$ is expected for a form factor mediated by the ρ-meson. With measurements of the differential cross section to precision of the order of 1% it will be possible to measure the rms radius of the pion and will also be possible to use the detailed shape of the differential cross section to distinguish among models giving the same rms radius.

The present proposal represents a re-thinking of earlier studies (See Appendices A and B) made in connection with planning for the NAL accelerator. We have modified these earlier proposals to improve the experiment in the light of suggestions which have since been made.

III. Experimental Arrangement

A. General Experimental Arrangement

1. Trigger:

The experimental layout is shown in Fig. 2. The experiment is designed to detect and measure 100 GeV/c π^+e^- elastic scattering events where the scattered electron has momentum in the range 20 to 84 GeV/c. The high-momentum high-resolution π^+ beam impinges on a 50 cm hydrogen target. Gas Cerenkov counters in the beam separate e^+ and (π^+, μ^+) from protons. A dE/dx counter, C1, upstream from the hydrogen target has a pulse-height requirement which will eliminate events with more than one charged particle ahead of the target. The π^+ and e^- from an elastic scattering event in the target travel forward as can be seen in Fig. 3 (π^+ maximum angle is 3.7 mrad, and the e^- maximum angle for the q^2-region of this experiment is 6 mrad). They pass through a hole in a lead-sandwich anti-counter, A1, surrounding the hydrogen target and through a hole in a similar anti-counter, A2, just in front of the magnet. A Cerenkov counter, C2, will signal the presence of an electron in the space between the target and the magnet. A thin dE/dx counter, C3, registers the existence of at least two minimum ionizing particles after the magnet. A hodoscope array, Hi, detects and roughly determines the positive particle momentum, p^+. Fast electronic logic requires a corresponding ($100-p^+$) GeV energy in the electron shower counter, S1. The discriminator windows that form this requirement are broad enough to be 100% efficient on real πe elastic scattering events. A pulse height greater than minimum in S2

signals a strongly interacting particle cascade shower.

Multiple anti-counters discriminate against other sources of background triggers. The combination of anti-counters A1 and A2 effectively eliminates any events with a charged particle or gamma produced at an angle > 10 mrad from the forward direction. Neutrons > 10 mrad will also be eliminated with reduced efficiency. The combination of anti-counters A3, A4, A5, and A6 will veto any event with a charged particle that makes it through the hole of A2 but which does not have a momentum > 20 GeV/c. No gamma anti-counters are placed at the center of the experiment in order a) not to complicate the radiative corrections which must be calculated to a good precision, and b) not to veto a good event with synchrotron radiation from the electron in the forward direction. Finally, a beam anti-counter, A7, vetos an event accompanied by a charged particle similar to a beam particle.

2. Wire Chambers:

Pairs of Charpak Chambers WC1, WC2, and WC3 are in an area where the high incident-beam intensity exists. Additional Charpak chambers will be placed upstream from the target. Chambers WC4 and WC5 (with a dead region for the beam) are ordinary magnetostrictive wire spark chambers. These chambers measure the incident-beam direction and the directions of the outgoing π^+ and e^- before and after the magnet. This will yield momenta and angles for all particles in the reaction, allowing a four-constraint fit (actually three effective constraints since energy and momentum are essentially identical at these energies).

B. The Target:

The ideal target for this electromagnetic experiment will have the maximum number of electrons (αZ) per effective nucleon ($\alpha A^{2/3}$) and per radiation length ($\alpha Z(Z+1)$). The former requirement is to maximize the ratio of the πe elastic scattering signal to the strong interaction background produced via nucleon interactions. The latter requirement is to minimize the Coulomb scattering and bremsstrahlung energy-loss effects. The length of various targets to achieve 10^{24} electrons/cm^2 is given in Table II below, with ensuing nucleon and radiation characteristics.

Table II

	$_1H^1$	$_{3}^{6.94}Li$	$_{4}^{9.01}Be$	$_7(CH)^{13}$	$_8(CH_2)^{14}$	$_4(LiH)^{7.95}$
ρ	0.0708	0.534	1.848	1.05	0.92	0.82
ℓ (cm)	23.6	7.20	2.04	2.96	3.18	3.32
ℓ/ℓ_r	0.0288	0.0487	0.0588	0.0718	0.0663	0.0362
10^{-24} x no. eff. nucleons/cm^2	1	1.21	1.09	0.894	0.907	1.17

Most of the listed materials are about the same in effective number of nucleons per electron, but hydrogen wins out in the fractional radiation length per electron. Since the bremsstrahlung energy-loss of the electron in the target is a serious problem in this experiment (and prohibits the use of a longer target) we have a chosen a hydrogen target. A length of 50 cm provides a compromise between counting rate and radiation length. Care must be taken in the design of the target so that its length (cold) and the density are each known to precisions better than the 1% goal of the experiment. Hydrogen for the target material has the additional advantage

of being neutron-free and will reduce, to some extent, the background trigger problem.

C. Counters:

1. dE/dx Counter:

Because of the large Landau tail on the high side of the pulse-height distribution for a single minimum-ionizing particle, the requirement that the pulse height in C1 be less than twice minimum will not include some valid beam particles. This loss is unimportant, however, since it occurs in a way which will not bias the physics results, and merely reduces the effective beam intensity slightly. The advantage of C1 is that it will effectively veto events similar (or identical) to real events which occur upstream of the hydrogen target, thus minimizing the target empty rate. Since it will be neccessary to do a target full and empty subtraction to get the answer for a precisely determined amount of target material, the statistical precision of the result will be thereby enhanced. We require a > 1 times minimum pulse height from counter C3. This requirement will be set low enough so that a very low percentage of the twice minimum real events will be missed.

2. Shower Counters:

The S1 shower counter will probably be a series of lead and lucite sheets similar in design to other counters that have been reported in the literature.[7] The electron energy resolution is expected to be better than $\sim 2\%$, and should easily distinguish electrons from π^-'s in the energy region of this experiment. The pulse heights will be loosely used in the fast trigger but will, in addition, be digitized and fed into the on-line computer as part of the data for the event (as will the pulse heights of the other counters).

Shower counter S2 may be identical with S1 or may have the lucite replaced with scintillator to enhance the response to π^+'s. It will be a trade-off of the desired π^+ response and the secondary tasks of identifying e^+'s and μ^+'s.

D. Backgrounds

The extreme forward production angles for π-e elastic scattering make possible the use of a target of small cross section which can be surrounded by anticoincidence counters to eliminate all but the most forward inelastic events. The identification of the electron in the electron shower counter allows elimination of all such events which do not have a high energy e^- associated with them.

An obvious source of spurious events would be processes of the type

$$\pi^+ + e^- \rightarrow \pi^+ + e^- + \pi^o\text{'s}.$$

The cross section for these processes is down by a factor of at least α from the elastic cross section so they should not present a large background in the trigger rate. Kinematic analysis should later eliminate most of the events of this type which might produce spurious triggers.

Another source of possible background might be strong interaction events such as

$$\pi^+ p \rightarrow \pi^+ p \pi^o$$

in which an electron pair is produced in the target, either by Dalitz decay of the π^o or by pair production from one of the π^o gammas. Only those events in which the negative electron carries a high fraction of the momentum not given to the π^+ would trigger the proposed experimental apparatus. No detailed information is available on pion production in the 100 GeV/c range, but data[8] at energies up to 25 GeV/c suggest that there will be a significant cross section for pion production with low momentum transfer to the nucleon. The fraction of events

which will appear kinematically similar to π-e elastic scattering (events can be eliminated by checking for coplanarity as well as energy balance,) is very small. But care must be taken to minimize the number of triggers produced by such backgrounds. This can be done by minimizing the number of radiation lengths of material in which the γ's can produce pairs and by using anticoincidence counters not only near the target but also downstream before, inside, and beyond the magnet to eliminate events with additional slow charged particles in the forward direction. We estimate that the number of triggers from this source will not be large compared to the number of true π^+e^- triggers. A further limitation on the spurious trigger rate may be attainable by using information from shower counters in both the π^+ and e^- legs of the spectrometer to require a crude energy balance for the event as part of the trigger.

E. Systematic Errors, Calibrations, and Internal Checks:

The desired goal of the experiment is to reduce statistical and systematic uncertainties in $d\sigma/dT_e$ to $\lesssim 1\%$. The usual problems of monitoring and distinguishing the π^+'s in the beam, the target length and density, the target empty rates, accidentals, etc., will have to be beat down. In addition, the dominant problems of (a) the radiative corrections and (b) background which simulates the πe elastic scattering events will have to be carefully treated. The radiative corrections (a) have been mentioned previously, and will have to be calculated by a theorist to the necessary precision with a calculation that is tailored to the details of the experiment. Several experts in this field exist in the U. S., and at least one has expressed an interest in performing the calculation.

The backgrounds (b) can be studied by studying the event rate as one applies the kinematical constraints in the fitting process. An additional check will be to study the $e^+ e^-$ and $\mu^+ e^-$ elastic scattering events that will occur along with the πe events due to e^+ and μ^+ contamination in the positive beam. Data on these processes will be taken simultaneously and can be separately analyzed. The radiative correction for $\mu^+ e^-$ should parallel $\pi^+ e^-$. The strong interaction background events in the $\mu^+ e^-$ case should be down $\sim \alpha$ from the π^+ case. The endpoint e^- energies from the $\mu^+ e^-$ and $e^+ e^-$ cases are 90 GeV and 100 GeV, respectively. Thus these processes will have finite cross sections at 84 GeV/c. The elastic reaction $e^+ e^-$ will have an energy loss by bremsstrahlung in the target three times larger on the average than

than either πe or μe. By studying the differences among these data, additional checks can be made on the theory and the experiment.

F. Running Time Estimates:

Assuming a 100 GeV/c beam intensity of 10^6 particles per pulse a π^+/p ratio of 0.2 from 200 GeV protons incident upon a Be target, a repetition rate of 900 pulses/hour, a hydrogen target of 50 cm, and an integrated πe elastic scattering cross section of 5.3 μbarns (assuming a point charge with no radiative corrections), the real event rate per hour will be

$(0.2 \times 10^6) \times (900) \times (50 \times 0.07) \times 5.3 \times 10^{-30} \times 6 \times 10^{23} = 2900$ events/hr.

A data-taking time of 500 hours with a combined efficiency of NAL + experiment of 0.7 will give 10^6 events. This should be further multiplied by additional factors of $\gtrsim 0.75$ and ~ 0.7 to account for the expected F^2 and radiative effects, respectively. The final physics result will produce the statistical precision shown in Fig. 4.

IV. APPARATUS

A. Items of Equipment Furnished by NAL.

1. An 18 kgauss 3-m long spectrometer magnet with power supply. An aperture at least 8 in high by 13 in wide is neccessary to include the full range of production angles and momenta which must be covered. The magnetic field integral must be known to better than 1/2 %. If necessary, the measurement of the magnet could be done by the experimenters.

2. A liquid hydrogen target of 2 in. diameter and 50 cm length. The target should have special provisions for very low boiling and for a measurement of its length (while cold) to achieve a known amount of hydrogen target material to a precision of better than 1%.

3. Miscellaneous items of electronics from PREP.

4. Beam Cerenkov counters. One should be capable of telling e^+ from everything, and another (π^+, μ^+, e^+) from p's.

5. Small amounts of time are needed on a large computer to completely analyze small fractions of the data during the progress of the run.

B. Items of Equipment to be Furnished by the Collaboration.

1. Charpak chambers and readout electronics. These chambers and the associated electronics are to be provided by the NAL part of the collaboration. They are necessary in regions where the beam is present, so that high beam intensity can be used. Since the angular divergence of the beam and of the secondary particles of interest is quite small, the chambers

in front of the magnet can be made quite small. A somewhat larger Charpak chamber is needed just after the magnet with dimensions slightly larger than the magnet aperture.

2. Magnetostrictive wire chambers and readout electronics. These chambers are to be provided by the Notre Dame part of the collaboration. Chambers and electronics which should be adequate already exist and have been operated by Notre Dame in experiment E-222 at Argonne National Laboratory. If wire planes of dimensions somewhat different from the existing chambers prove desirable, they can easily be provided.

3. Varian Data 620-i computer and magnetic tape transport. These items will be provided by Notre Dame together with the interface connecting the computer with the chambers and counters. The computer and tape transport are currently being used by Notre Dame in an experiment at ANL. Interfaces to magnetostrictive chambers and hodoscope counters are operative. Additional interface electronics will be purchased or constructed.

4. Electronics trailer. An electronics trailer now being used by Notre Dame at ANL will be used for this experiment.

5. Shower counter. Two shower counters and associated electronics must be constructed. The responsibility is to be shared by the collaborators. Similar shower counters[7] have been used successfully to discriminate between electrons and pions in connection with the SLAC 20 GeV spectrometer, thus demonstrating the feasibility of the technique.

6. Miscellaneous counters. The responsibility for constructing and testing other neccessary counters, dE/dx counters, anti-coincidence counters, and the Cerenkov counter downstream from the target is to be shared between the collaborators. Notre Dame already has some stocks of phototubes, etc., which may be utilised in the construction.

It is to be expected that all equipment will be ready in advance of the first round of experiments at NAL.

FIG. 1 CROSS SECTION

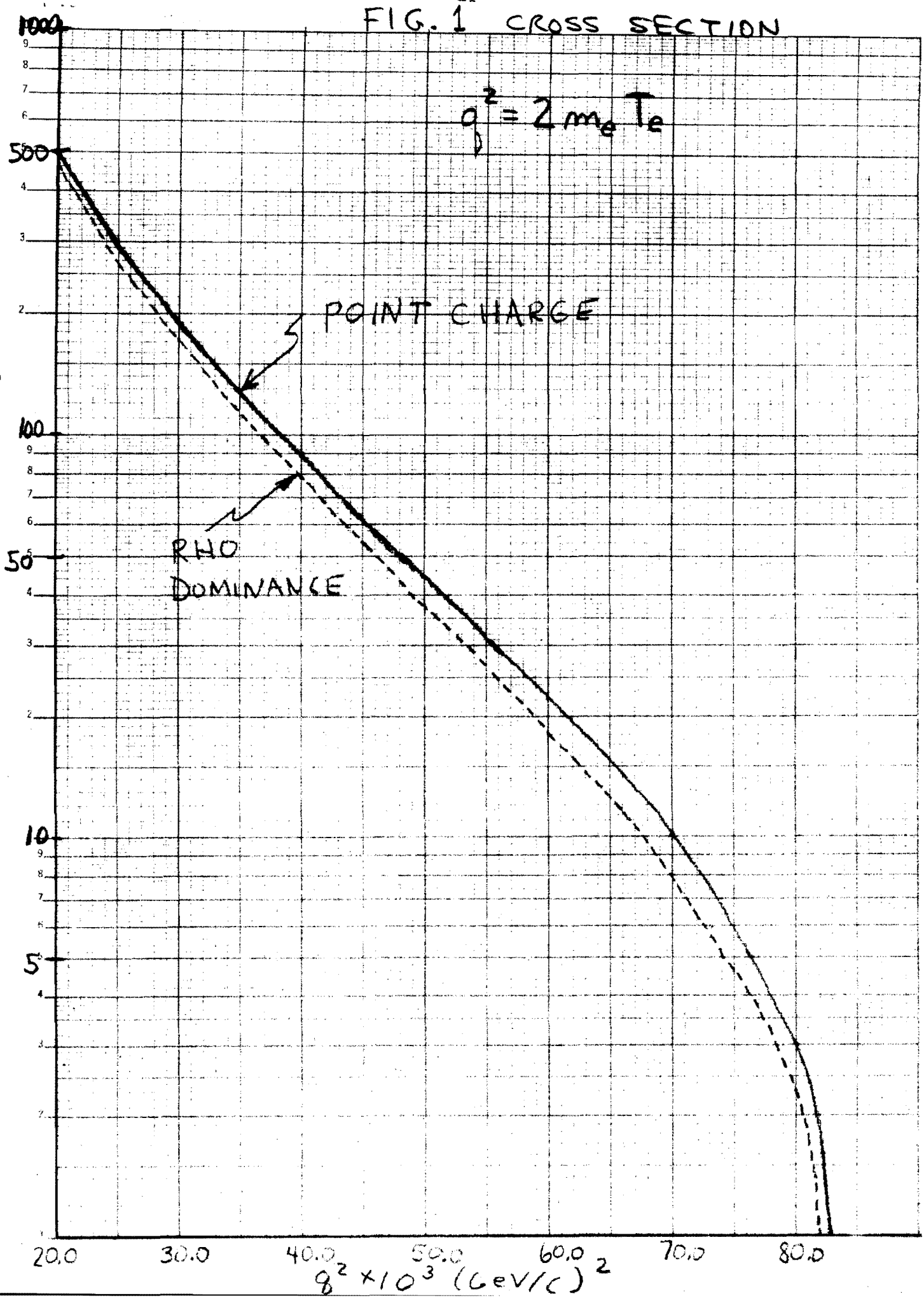

FIG. 2 $\pi^+e^- \rightarrow \pi^+e^-$ EXPERIMENTAL LAYOUT

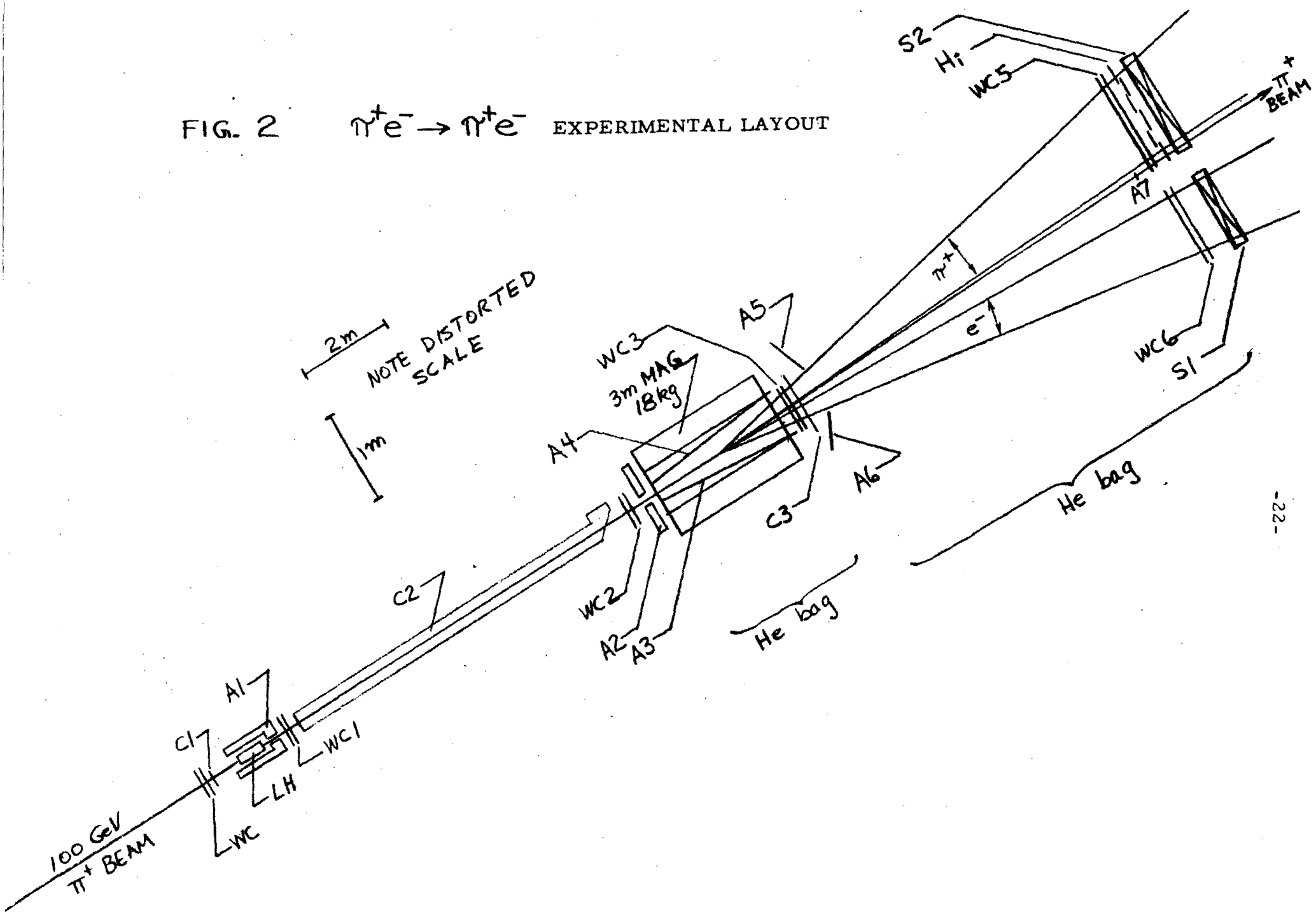

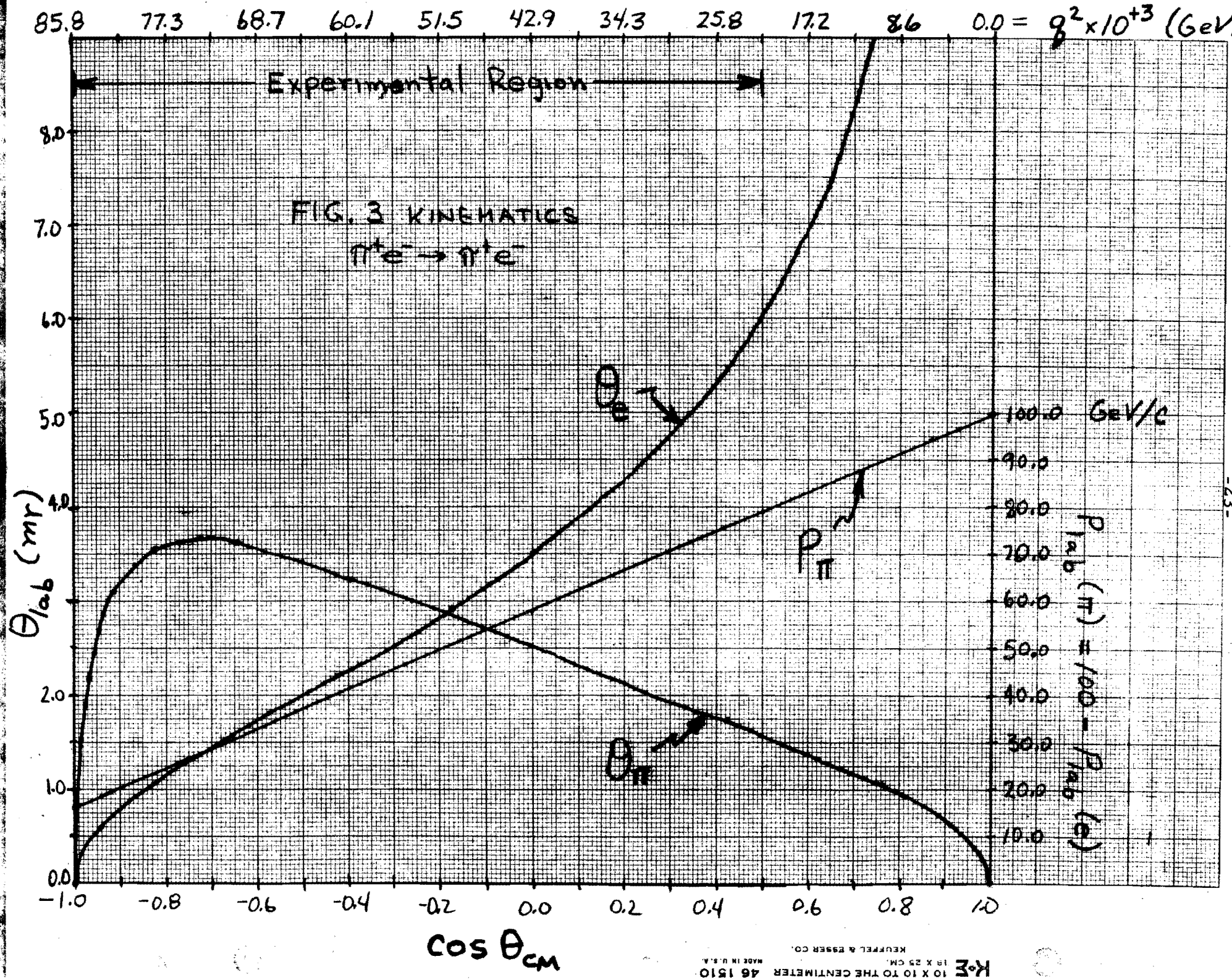

FIG. 4 PHYSICS RESULTS

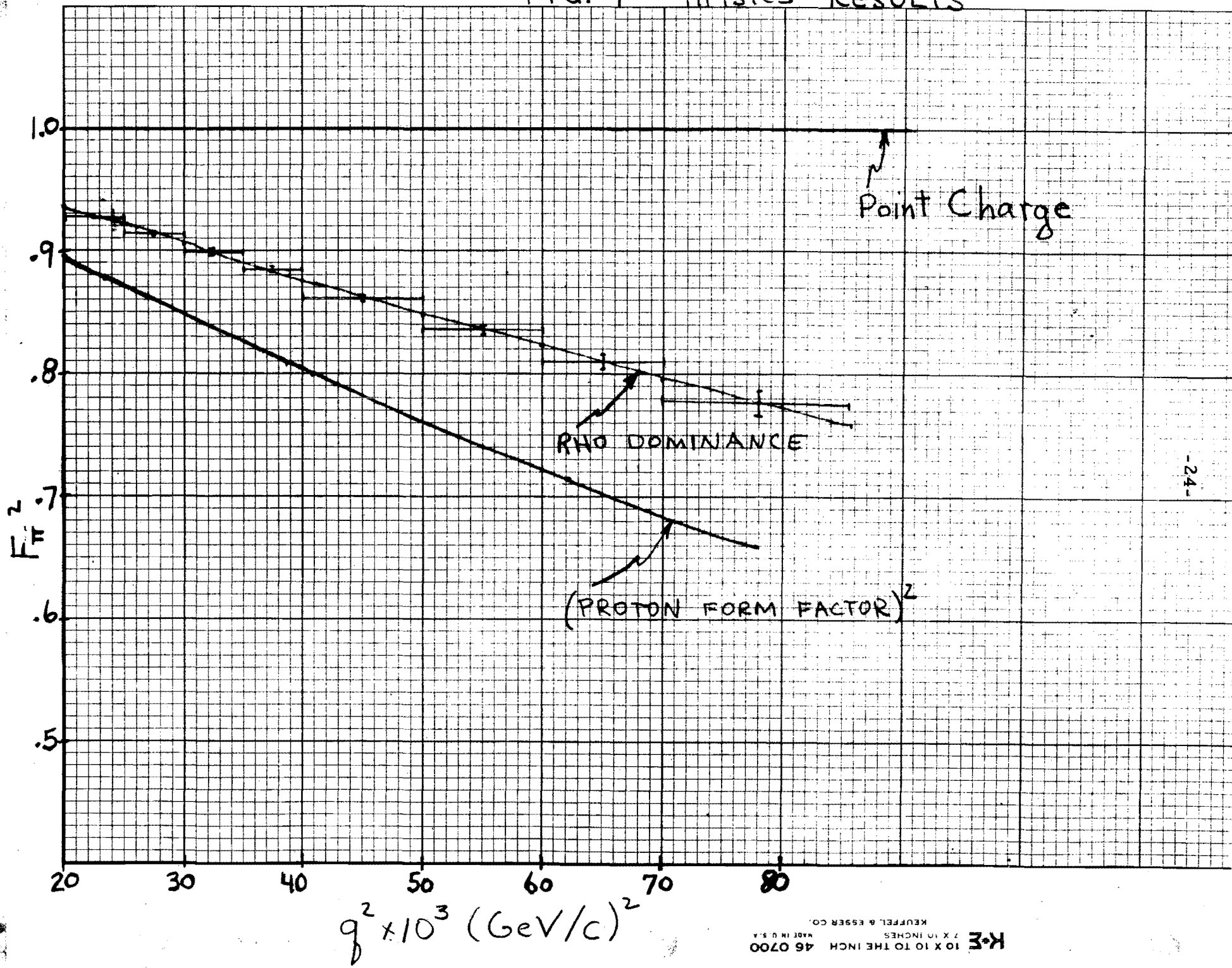

References

1. F. Crawford, Phys. Rev. 117, 1119 (1960) and UCID-241 (1957), unpublished.
2. (a) J. Allen, G. Ekspong, P. Sallstrom, and K. Fisher, Nuovo Cimento 32, 1144 (1964). (b) D. Cassel, M. Barton, R. Crittenden, V. Fitch, and L. Leipuner, (to be published).
3. M. M. Block, Phys. Letters 25B, 604 (1967); M. M. Block, I. Kenyon, J. Karen, D. Koetke, P. Malhotra, R. Walker, and H. Winzeler, Phys. Rev. 169, 1074 (1968).
4. C. Mistretta, D. Imrie, J. A. Appel, R. Budnitz, L. Carroll, M. Goitein, K. Hanson, and Richard Wilson, Phys. Rev. Letters 20, 1523 (1968).
5. H. J. Bhabha, Proc. Roy. Soc., A164, 257 (1938).
6. See, for example, J. Kahane, Phys. Rev. 135, B975 (1964), L. W. Mo and Y. S. Tsai, Rev. Mod. Phys. 41, 205 (1969), and L. C. Maximon, Rev. Mod. Phys. 41, 193 (1969). Extensive bibliographies are contained in these references.
7. See, for example, C. A. Heusch and C. Y. Prescott, IEEE Transactions on Nuclear Science, NS-12, No. 4, 213 (1965).
8. W. D. Walker, etal. Phys. Rev. Letters 20, 133 (1968).

Appendix A

APPENDIX A. Pages 144 through 157 of "DESIGN STUDY 200 Bev Accelerator:Studies on Experimental Use,Vol I,1964-5,LRL,Berkeley,Calif

Rev. September 30, 1964
UCID-10125
AS/Experimental/02
August 20, 1964
Timothy E. Toohig

AN EXPERIMENT TO MEASURE THE PION FORM FACTOR AT THE 200 GeV ACCELERATOR

A. Introduction

Considerable information about the electromagnetic structure of nucleons has been obtained in recent years from electron-nucleon scattering experiments.[1,2,3] It is of interest to obtain similar information about other particles, and in particular about the π-meson.

Since the pion is an unstable particle with a lifetime of 2.6×10^{-8} sec, it cannot be used as a target in the sense of the nucleon in e-p scattering. It is necessary to use the inverse of the electron-nucleon scattering procedure to probe the pion structure. In this process beam pions are scattered off target electrons in a hydrogen bubble chamber or target. Crawford[4,5], in 1960, carried out such an experiment using 1.12 GeV/c π^- mesons incident on a hydrogen bubble chamber at the Lawrence Radiation Laboratory, Berkeley. An Aachen-Stockholm collaboration[6] has done a similar experiment using 16 GeV/c π^- mesons in a CERN hydrogen bubble chamber. Fitch and Leipuner[7] have recently completed a spark-chamber experiment at Brookhaven using 20 BeV/c π^- mesons to obtain higher statistics for the process. Crawford[4] has pointed out that significant structural effects are not expected to begin to appear until the deBroglie wavelength of the target electron in the rest system of the bombarding pion is less than the Compton wavelength of the pion. This condition obtains at a pion laboratory momentum of 38 GeV/c. Longo[8] estimates a flux of 10^7 pions/sec at 150 GeV/c, considerably beyond the 38 GeV/c criterion, from a proposed pion beam at the 200 GeV AGS. This flux, calculated from Keefe's[9] estimates of particle production in the 200 GeV machine, is adequate for a π-e scattering experiment at this energy.

As pointed out by Ford and Hill,[10] the Born approximation for the electron-nucleon scattering is the simplest approach to obtain at least qualitative insight into the effect on electron scattering of the size and radial shape of the charge distribution within the nucleon. A similar analysis is valid for the pion. In the Born approximation the cross-section is proportional to the square of a form factor, F.

i.e.

$$\left(\frac{d\sigma}{dT}\right)_{\text{measured}} = F^2(\Delta^2)\left(\frac{d\sigma}{dT}\right)_{\text{point charge}} \qquad (1)$$

where $\Delta^2 = 2 m_e T$ (1a)

$=$ the 4-momentum transfer to the scattered electron.

$T =$ the kinetic energy of the scattered electron.

To a first approximation F^2 is related to the rms radius of the pion by

$$F^2 = 1 - \frac{\langle r^2 \rangle}{3} \Delta^2 \qquad (2)$$

The rms radius of the pion can be obtained from the experimental determination of the π-e scattering cross-section by determining the best fit of the function given by Eq.(2) to the experimental ratio

$$\left(\frac{d\sigma}{dT}\right)_{\text{meas.}} / \left(\frac{d\sigma}{dT}\right)_{\text{point charge}}$$

Some insight into the structure of the pion can be gained by postulating that the form factor, F, is mediated by a meson of mass m_{ff} so that

$$F^2 = \left(\frac{m_{ff}^2}{\Delta^2 + m_{ff}^2}\right)^2 \qquad (3)$$

The value of m_{ff} is expected to be close to the mass of the ρ-meson, thus $m_{ff}^2 \approx 0.5\ (\text{GeV})^2$. Curves of the type given in Fig. 1 can be constructed for various values of m_{ff} and fitted to the experimental data to determine the mass of the particle responsible for the structure of the π-meson, if structure is observed.

B. Cross Sections and Kinematics

The interaction of charged particles with atomic electrons has been treated extensively in considerations of the stopping power of materials for charged particles.[10,11,12,13] Pauli[14] has obtained a very complete set of cross-sections and angular distributions derived from field theory. The pertinent relation here is that for the cross-section per unit energy for production by incident spin-zero particles of knock-on electrons,

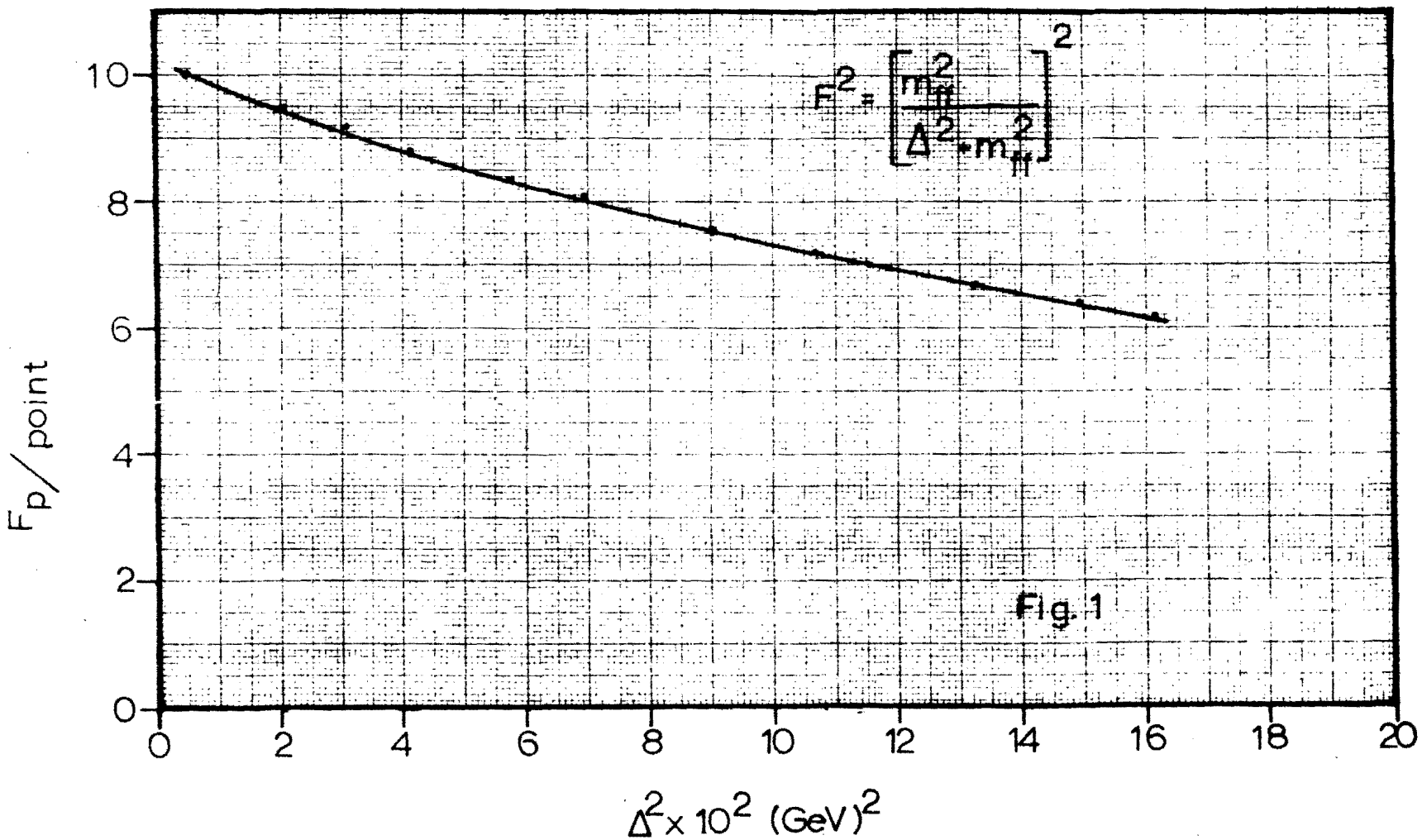
$F^2 = \left[\frac{m_{\pi\pi}^2}{\Delta^2 + m_{\pi\pi}^2}\right]^2$
F_p/ point
$\Delta^2 \times 10^2$ (GeV)^2
0
2
4
6
8
10
12
14
16
18
20

Fig. 1

$$\frac{d\sigma}{dT} = \frac{2\pi m_e r_e^2}{\beta^2} Z \frac{1}{T^2} \left[1 - \beta^2 \frac{T}{T_{max}} \right] \text{cm}^2/\text{atom} \qquad (4)$$

where m_e, r_e = the electron mass and classical radius

T = the laboratory kinetic energy of the scattered electron

T_{max} = the maximum possible value of T for a given incident particle momentum.

$$= 2 m_e \left(\frac{p^2}{m_e^2 + m^2 + 2 m_e \epsilon} \right)$$

p, m, ϵ, β = the laboratory momentum, mass, total energy and velocity of the incident particle

Z = the atomic number of the target material.

The total cross-section, $\sigma (T_{min} \leq T \leq T_{max})$, where T_{min} is an arbitrary lower limit of T, is given by:

$$\sigma (T \geq T_{min}) = \int_{T_{min}}^{T_{max}} \frac{d\sigma}{dT} dT = \frac{2\pi m_e r_e^2}{\beta^2} Z \left[\frac{1}{T_{min}} - \frac{1}{T_{max}} - \frac{\beta^2}{T_{max}} \ln \left(\frac{T_{max}}{T_{min}} \right) \right] \frac{\text{cm}^2}{\text{atom}} \qquad (5)$$

These cross-sections are based on point-charge calculations. For an extended pion the cross-section as given by Eq.(4) is modified by a form factor as given in Eq.(1). Typical results of the cross-section calculations are given in Table I for two values of incident pion momentum.

TABLE I

p_{inc}(GeV/c)	T_{min}(GeV)	T_{max}(GeV)	$\sigma(T > 5$ GeV)	$\lambda(\frac{\hbar}{m_\pi c})^*$	Interaction Length (m)
100	5	83.96	3.93 mb	0.24	6.03×10^3
150	5	133.05	4.27 mb	0.16	5.55×10^3

* λ is the deBroglie wavelength of the electron in the pion rest system in units of the Compton wavelength of the pion.

Figures 2 and 3 illustrate the variation of $\frac{d\sigma}{dT}$ with 4-momentum transfer, Δ^2 for incoming pion momenta of 100 and 150 GeV/c respectively, and for various values of m_{ff} in the form factor.

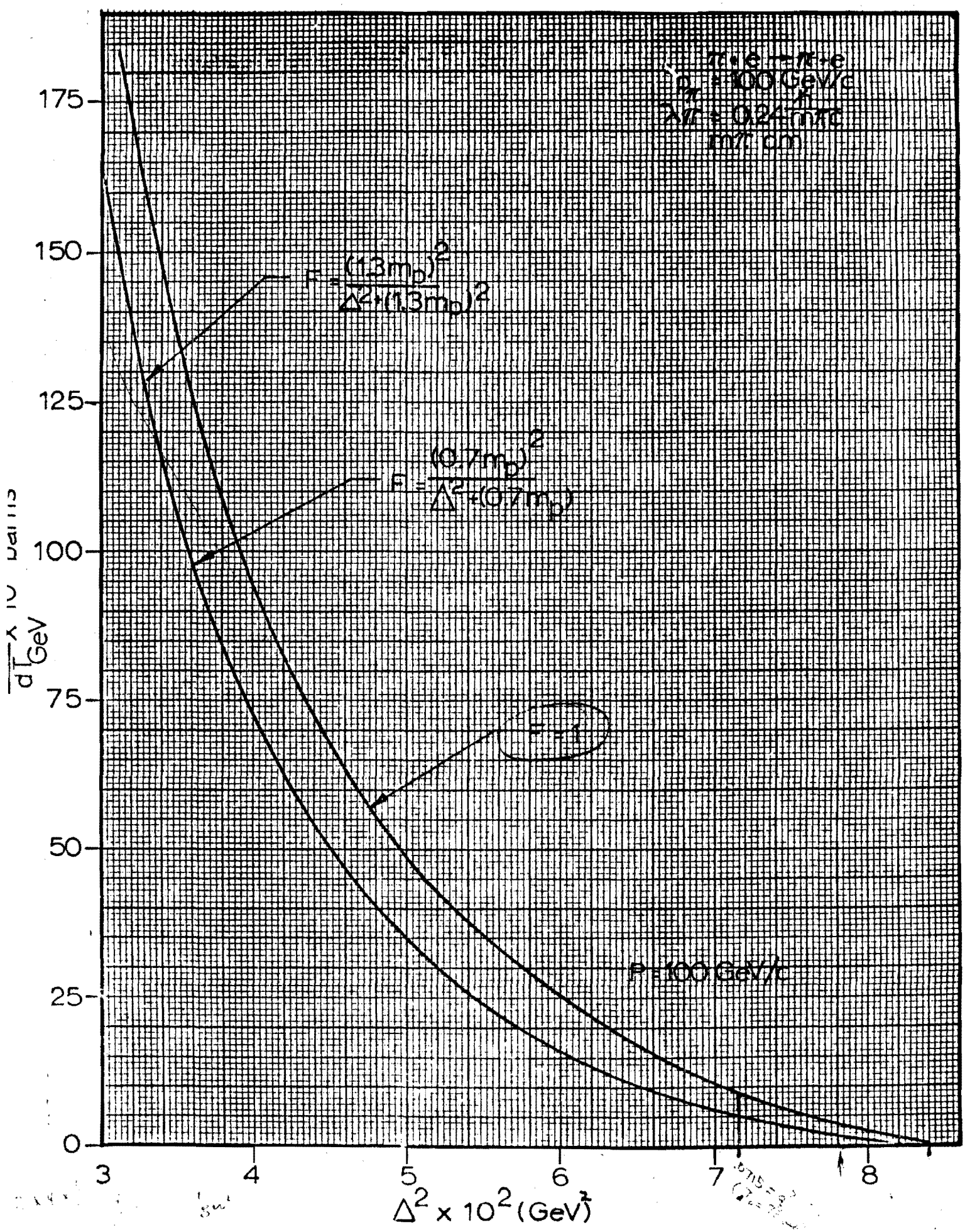
$\pi \cdot e \to \pi \cdot e$
$p_\pi = 100\ GeV/c$
$\lambda_{\pi^-} = 0.24\ fm$
$m_\pi = m_\pi$
$F = \frac{(1.3m_p)^2}{\Delta^2 + (1.3m_p)^2}$
$F = \frac{(0.7m_p)^2}{\Delta^2 + (0.7m_p)^2}$
$F = 1$
$P_\pi = 100\ GeV/c$
$\frac{d\sigma}{d\Delta^2} \times 10^{38}\ \frac{cm^2}{GeV^2}$
$\Delta^2 \times 10^2\ (GeV)^2$
0
25
50
75
100
125
150
175
3
4
5
6
7
8

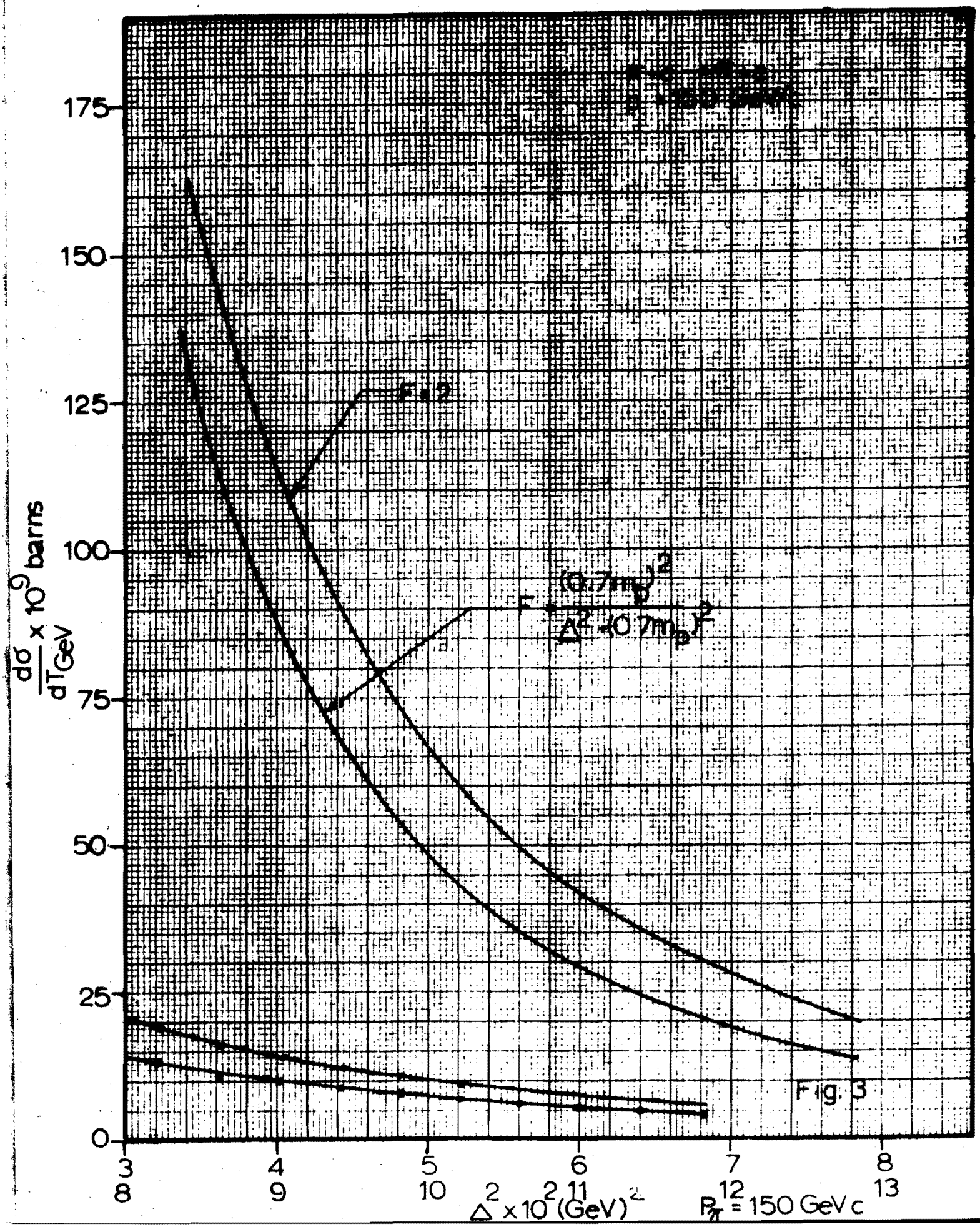
175
150
125
100
75
50
25
0
$\frac{d\sigma}{dT}$ GeV x 10^{9} barns
F=2
$F=\frac{(0.7m_p)^2}{\Delta^2-(0.7m_p)^2}$
3
8
4
9
5
10
6
11
7
12
8
13
$\Delta^2 \times 10^2 (GeV)^2$
P_T = 150 GeV c

Fig. 3

C. Experimental Layout and Energy Loss Considerations

(a) Experimental Layout

From Figs. 2 and 3, three effects are noteworthy: (1) the maximum attainable value of the 4-momentum transfer to the target electron, Δ^2_{max}, is a function of the incident pion momentum; (2) for a given Δ^2 the flux, $\frac{d\sigma}{dT}$, increases with increasing incident pion momentum, (3) the fractional deviation of the form factor, $F(m_{ff})$, from the point charge value $F(1)$, increases with increasing Δ^2. All of these reasons indicate an experiment at the highest practicable incident pion momentum. Figure 4 is a proposed experimental arrangement for an incident pion momentum of 100 GeV/c.

To achieve spatial separation of the final-state pion and electron at the detector, it is required that

$$p_{min}(\text{electron}) = p_{max}(\text{pion}) = \frac{1}{2}\, p\,(\text{incident}) \qquad (6)$$

This condition is illustrated in Fig. 4 for the 100 GeV/c beam. π-mesons of momentum 100 GeV/c are incident on the 1 meter hydrogen target, where they will produce ~ 5 interactions/10^6 pions with $T_{electron} > 50$ GeV.

Tables II and III give the relevant parameters and kinematics for a 100 GeV/c and a 150 GeV/c experiment satisfying Eq.(6).

TABLE II*

p_{inc}(GeV/c)	T_{min}(GeV)	T_{max}(GeV)	$\sigma(>T_{min})$	Δ^2_{max}(GeV)^2	Interaction Length	Events/day with $T_{el}>T_{min}$
100	50	84	0.49 μb	.084	4.9×10^5	4×10^5
150	75	133	0.38 μb	.135	0.62×10^6	5×10^4

* Assuming 10^6 pions/sec in the beam

TABLE III

p_{inc}(GeV/c)	$p_{e\ min}$(GeV/c)	$p_{e\ max}$(GeV/c)	$\theta_{e=\pi}$	$p_{\pi\ min}$(GeV/c)	$p_{\pi\ max}$(GeV/c)
100	50	84	0.165°	16	50
150	75	133	0.14°	17	75

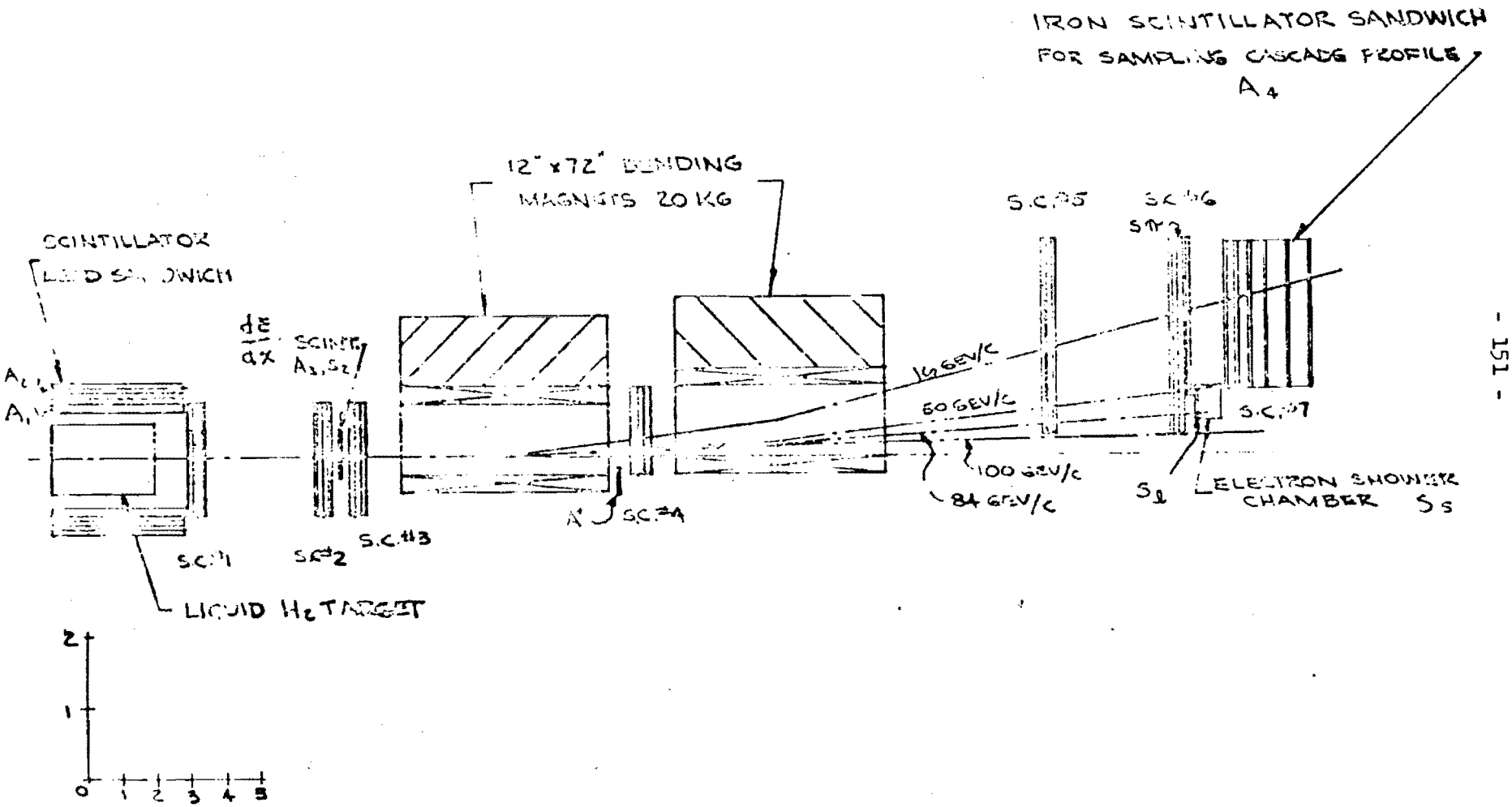

PION FORM FACTOR EXPERIMENT

Fig. 4

The scintillator sandwich, A_1, A_2 surrounding the target is in anti-coincidence to discriminate against events producing charged particles, neutrons or gammas other than in the forward direction. A_3 discriminates against slow charged particles produced in the forward direction. S_2 specifies tracks with $\frac{dE}{dx} >>$ minimum. The subsequent spark chambers define the particle trajectories through the bending magnets for momentum determination. The simultaneous passage of two charged particles is signalled by coincidence in S_π, S_e. Particle identification is accomplished by requiring a shower in S_5 and a μ-meson anti-coincidence in A_4, an Fe-scintillator sandwich which samples the growth of the nuclear cascade.

The experiment is extremely simple in principle. To determine the pion form factor dependence, m_{ff}, and the rms radius of the pion, it is only necessary to identify the pion and electron and measure the kinetic energy of the electron. The 4-momentum transfer, Δ^2, is then given by Eq.(1a). In practice, the magnitude of, and straggling in, the energy loss of the electron on traversing the system make the determination of the electron energy at production more difficult. A detailed consideration of the various energy loss factors follows. In contrast to other experiments, particularly at lower energies, there are no adverse solid angle factors; because both π and electron travel straight forward all useful events can be captured into the analyzing system.

(b) Scattering and Energy Loss Considerations

(1) Scattering of the final-state particles:

Since we are using "thin" targets and detectors, scattering of the particles will be governed by plural scattering considerations.[11] Figure 5 gives the average probability, Q, as a function of scattering angle for particles of various momenta calculated by the method of Snyder and Scott (ref. 11, p.73 ff). For a 25 GeV/c particle the scattering angle θ_y and $Q = Q_{max}/2$ is, from Fig. 5

$$\theta_y \ (Q = Q_{max}/2) \ = \ 0.14 \text{ mr}$$

(2) Energy loss considerations for the final-state particles:

The outgoing particles will lose energy by Bremsstrahlung and direct pair production in the target and the spark chamber plates and by synchrotron radiation in the bending magnets. These losses will be negligible for the pions, so what follows treats of the outgoing electron. A calculation of the fractional energy loss/gm cm^{-2} due to direct pair production yields a value of $\sim 10^{-5}$ over the energy range of interest. This loss is negligible.

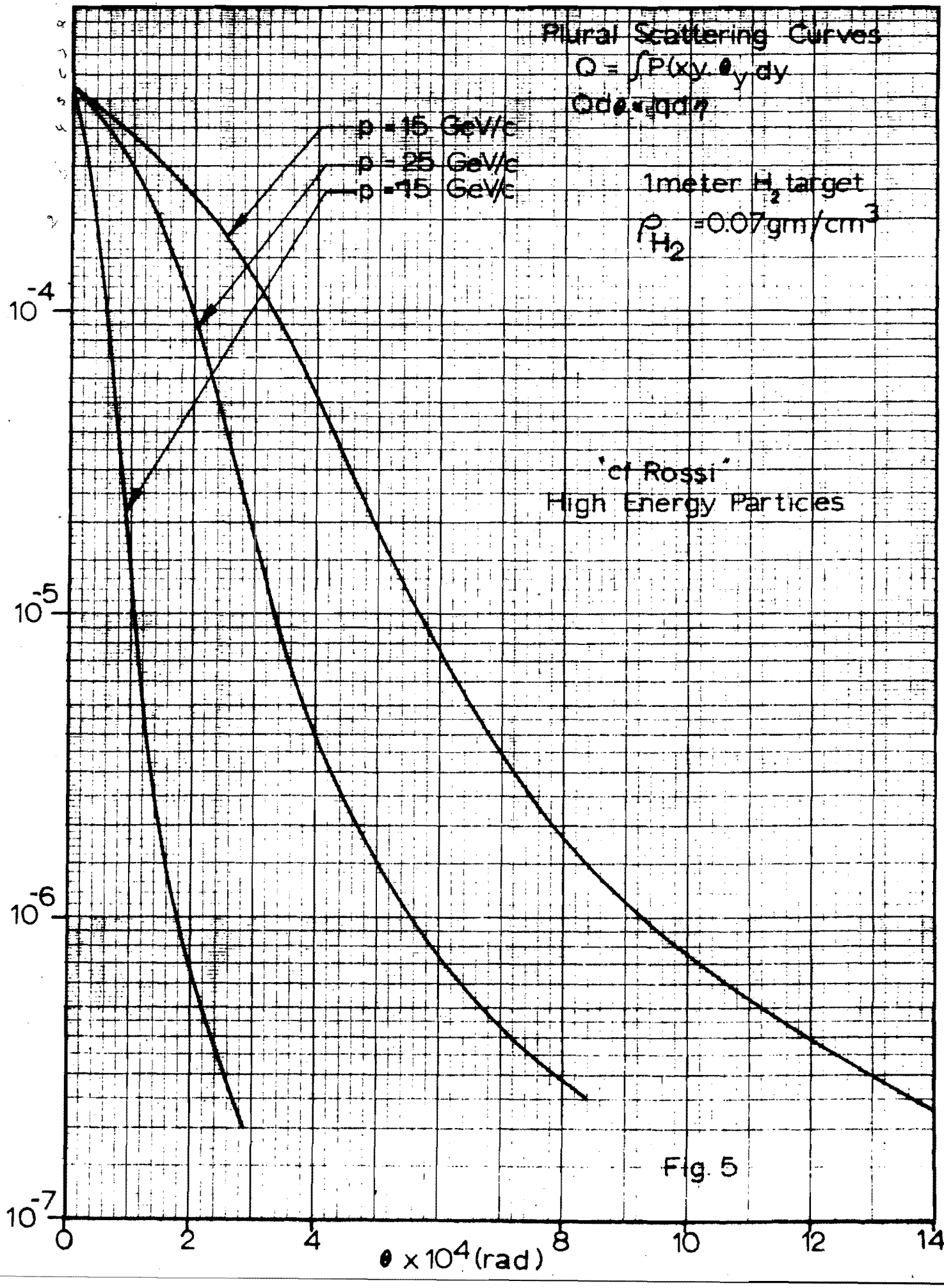
Plural Scattering Curves
$Q = \int P(xy.\theta_y\, dy$
$Qd\theta = \frac{1}{2}qd\eta$
p = 15 GeV/c
p = 25 GeV/c
p = 45 GeV/c
1meter H_2 target
ρ_{H_2} =0.07gm/cm^3
"cf Rossi"
High Energy Particles
10^{-4}
10^{-5}
10^{-6}
10^{-7}
0
2
4
8
10
12
14
$\theta \times 10^4$ (rad)

Fig. 5

The radiative (Bremsstrahlung) energy loss is given by[11,12,15]

$$\left(\frac{dT}{ds}\right)_{rad} = n\,(T + m_e)\,\sigma_{rad} \text{ energy units/cm} \qquad (7)$$

where

s = the distance travelled in the medium.

n = the number of atoms/cm^3 in the medium,

T = the kinetic energy of the electron in appropriate energy units.

$\sigma_{rad} = 4\,[\ell n\,(183\,Z^{-1/3}) + 1/18]\,\sigma_o\,Z^2$, for the extreme relativistic case with complete screening

or

$$\left(\frac{dT}{ds}\right)_{rad} \simeq \frac{\rho T}{X_o} \qquad T \gg m_e \qquad (8)$$

where

ρ = the density of the medium

$\frac{1}{X_o} = 4\,\alpha\,\frac{N}{A}\,Z^2\,r_e^{\,2}\,\ell n\,(183\,Z^{-1/3})$ = (the radiation length)$^{-1}$

For the hydrogen target, the average energy loss per cm is given by

$$\left(\frac{dT}{ds}\right)_{rad} = 0.84 \times 10^{-3}\ T \text{ GeV/cm} \qquad (9)$$

The energy loss due to synchrotron radiation in the two bending magnets is given by[15]

$$\left(\frac{dT}{ds}\right)_{synch.} = 1.27 \times 10^{-5}\ H_{kG}^{\ 2}\ T_{GeV}^{\ 2} \text{ MeV/m} \qquad (10)$$

where

H = the field in the bending magnet.

Table IV summarizes the pertinent energy loss considerations for the experimental setup of Fig. 4.

TABLE IV (a)*

E_o = 100 GeV

T_{el}(GeV)	ΔT_{Brems}(GeV)	$\Delta T_{synch.}$(GeV)	ΔT_{pair}(GeV)	$F_{m\rho}/F_{point}$
50	2.1	0.050	$\sim 5 \times 10^{-4}$	84%
25	3.5	0.143	$\sim 3 \times 10^{-4}$	76%

* Assuming that, on the average, the interaction occurs at the midpoint of the target.

TABLE IV (b)

E_o = 150 GeV

T_{el}(GeV)	ΔT_{Brems}(GeV)	$\Delta T_{synch.}$(GeV)	ΔT_{pair}	F_{mp}/F_{point}
75	3.2	.114	$\sim 7.5 \times 10^{-4}$	79%
133	5.7	.360	$\sim 1.3 \times 10^{-3}$	64%

D. Background and Energy Loss Corrections

The extreme forward production angles for the π-e scattering make possible a target of small cross-section. The scintillator sandwich surrounding the target then discriminates against all but the most forward inelastic events. Scintillator A^+, after the first bending magnet, discriminates further against events in which a positive particle is produced. Using a negative pion beam, it is difficult, with these safeguards to simulate a good event. The net charge for the nuclear interaction is 0, while the experimental setup requires a net charge of -2. The only obvious source of spurious events is:

$$\pi^- + e^- \rightarrow \pi^- + e^- + \begin{cases} \gamma \\ \pi^o \end{cases} \qquad (11)$$

The Q-value for this reaction with π^o is 70 MeV at 100 GeV/c incident pion momentum, and 135 MeV at 150 GeV/c. The cross-section for these is down by at least α from the elastic cross-section. Some rejection of such inelastics can be had by requiring coplanarity of π and e within the limits of the plural scattering uncertainty.

The very sizeable probable energy loss due to Bremsstrahlung given in Table IV can be corrected by two independent approaches. The first is to require energy conservation between the initial and final states from a measurement of the final state pion energy and knowledge of the beam energy. Secondly, the electron spectrum as a function of Δ^2 can be determined. Heitler[16] gives the probability distribution for the decrease in energy of an electron after traversing matter of a finite thickness ℓ.

$$w(y)\,dy = \frac{e^{-y}\, b\ell - 1}{\Gamma(b\ell)}\, dy \qquad (12)$$

where $y = \ell n\,[T_o/(T_o - \Delta T)]$

ΔT = the loss of energy.

The parent distribution for a given number of electrons with the same measured energy can be unfolded using Eq.(12). The plot of $N(\Delta^2)$ vs Δ^2 as determined from this unfolding must agree with that determined from energy balance on the initial and final state pions.

As a check on the method, the bending magnets can be reversed and their fields appropriately changed for proton-electron scattering. The proton form-factor is well known in the range of 4-momentum transfer accessible in this setup, i.e. $\Delta^2 < 0.038$ $(GeV)^2$.

E. Conclusions

With presently known techniques it is possible to explore the structure of the pion with good statistics down to distances of the order of 1/6 of the Compton wavelength of the pion. This corresponds to a maximum 4-momentum transfer of 0.135 $(GeV)^2$. From the data it should be possible to determine the shape of the differential cross-section for 4-momentum transfer to the electron to the order of 1%. In the region of 4-momentum transfer accessible to the proposed experiment, a form factor mediated by the ρ-meson departs from the point charge form factor by up to 30%.

With the availability of K^- and μ^- beams of sufficient intensity up to a beam momentum of 100 GeV/c the same basic experimental arrangement is suitable for probing the μ and K form factors out to 4-momentum transfers of 0.091 $(GeV)^2$ and 0.030 $(GeV)^2$ respectively.

km

REFERENCES

1. K. W. Ford and D. L. Hill, Annual Reviews of Nuclear Science, Vol. 5 (Annual Reviews, Inc., Palo Alto, Calif., 1955).

2. R. Hofstadter, Annual Reviews of Nuclear Science, Vol.7 (Annual Reviews, Inc., Palo Alto, Calif., 1957).

3. R. Herman and R. Hofstadter, High Energy Electron Scattering Tables, (Stanford University Press, Stanford, Calif., 1960).

4. F. Crawford, Physics Review 117, 1119 (1960).

5. F. Crawford, UCID-241 (1957), (unpublished).

6. J. Allan, G. Ekspong, P. Sallstrom, K. Fischer (to be published).

7. V. Fitch, L. Leipuner (private communication).

8. M. Longo, "150 GeV/c Beam for Spark Chamber Experiments," LRL AS/Experimental/02, July 30, 1964.

9. D. Keefe, "Experimental Areas and Facilities," LRL AS/Experimental/02 February 22, 1964.

10. B. Rossi, K. Greisen, Reviews of Modern Physics, 13, 243 (1941).

11. B. Rossi, High Energy Particles (Prentice Hall, Inc., New York, 1952).

12. R. D. Evans, The Atomic Nucleus (McGraw - Hill Book Co., Inc., New York, 1955).

13. N. Mott, H. Massey, The Theory of Atomic Collisions, 2nd Ed. (Clarendon Press, Oxford, 1952).

14. W. Pauli, Reviews of Modern Physics, 13, 203 (1941).

15. D. Ritson, Techniques of High Energy Physics, (Interscience Publishers, Inc., New York, 1961).

16. W. Heitler, The Quantum Theory of Radiation, 3rd Ed. (Clarendon Press, Oxford, 1954).

Appendix B

APPENDIX B. Pages 49 through 56 of "The Electromagnetic Form factor of the charged Piom(muon,kaon,electron),1968 summer study,NAL C. 1-68-10

THE ELECTROMAGNETIC FORM FACTOR OF THE CHARGED PION (MUON, KAON, ELECTRON)

J. A. Poirier
University of Notre Dame

Introduction

Extensive work has been invested in understanding the electromagnetic form factor, EFF, of the proton in the space-like region and also in the time-like region. The ρ, ω, and ϕ should contribute to this form factor but do not predict the q^{-4} fall off of the EFF at high q. The charged pion EFF should be understood in terms solely of the ρ meson; thus it should be a much simpler beast to treat theoretically.

Different techniques have been employed in the past to obtain the EFF of the pion. Table I lists the results. Theory predicts the following behavior:

$$\text{EFF}(\pi) = \left(1 + q^2/m_\rho^2\right)^{-1}$$

which would give $r_\pi = 0.63 \times 10^{-13}$ cm. We propose a direct measurement of EFF (π) via elastic electron scattering using atomic electrons as the target material in a beam of high momentum pions.

Experiment

Liquid hydrogen is an ideal target since it will maximize the number of electrons per nucleon and also number of electrons per radiation length. The number of nucleons should be kept low to minimize the

background of strongly interacting processes; the number of radiation lengths should be kept low to minimize the bremsstrahlung energy loss of the recoil electron.

The available 100-GeV π^+ beams at NAL might have π^+ intensities in the beam $\sim 5 \times 10^7$/burst with 3 to 4 times as many protons. If all counters and spark chambers could be kept out of the main beam, full utilization of this intensity might be realized. Two things speak against this approach, however:

1. The number of strong interactions in the hydrogen target are about 6%; one begins to be limited by the rate in the anticounters.
2. The desired cross section is high enough that the running time does not become excessive even if the incident beam is lowered to $\sim 10^6$/pulse.

A midway philosophy is shown in Fig. 2 with two wire chambers in the beam as if the intensity were lowered but with an extra bending magnet in the electron arm of the spectrometer so that all variables of the π^+ and e^- can be obtained without any information from the wire chambers in the beam. Thus if the background problems are not severe, one might use this technique without the first two wire chambers in the beam to study the end point of the spectrum where the cross section becomes zero and to study the μ^+, e^+, and K^+ scattering from e^-'s where the fraction of these particles in the beam might be appreciably lower than the π^+'s.

The region of available momentum transfer q via this technique is limited. One should easily obtain the rms radius of the pion defined as

$$R_\pi^2 = \sqrt{< r^2 >} = -6 \frac{d}{dq^2} EFF(\pi) \Big|_{q^2 = 0} .$$

The range of q may be high enough that one can distinguish among models which have the same R_π. For example

$$EFF = e^{-\frac{1}{6} q^2 R_\pi^2} , \qquad (1)$$

and

$$EFF = \left(1 + \frac{1}{6} q^2 R_\pi^2\right)^{-1} , \simeq 1 - \frac{1}{6} q^2 R^2 \qquad (2)$$

will have the same slope at $q^2 = 0$ but (1) gives an effect of 0.756 at the maximum available q^2 while (2) gives 0.770 each with $R_\pi^2 = 6/m_\rho^2$ $= (0.62\ f)^2$. Thus an experiment of statistical precision of < 1% could tell the difference between these two shapes which are characterized by the same rms radius. Figure 1 shows the maximum available kinematic quantities for various incident particles as a function of incident momentum.

The incident beam is focused to a 1 cm spot with 0.1 mrad angular divergence as it enters the LH target. This is sufficiently precise that no additional measurement need be made. Anticounters around the target insure that the charged products of a reaction are well collimated in the forward direction. Wire spark chambers measure the angle and position of the π^+ and e^- particles after they have been bent away from

the incident beam. The electron's momentum is measured, its identity finally determined by a lead-scintillator counter sandwich. The trigger will be

1. no anticounters being triggered
2. a charged + strongly interacting particle
3. a negative electron.

The final fit to the event will be a 4c fit (overconstrained by 4 equations) with all quantities in the initial and final state particles measured or known. (A 4c fit at high energies, however, becomes effectively a 3c fit.)

$T_{e\,max}$ for 100-GeV/c incident π^+ is 84 GeV. The maximum momentum transfer, q_{max}, is

$$q_{max} = \sqrt{-t_{max}} = \sqrt{2\,M_e\,T_{e(max)}} = 0.29 \text{ GeV/c} .$$

The experiment covers a range of momentum transfers from q (max) to 1/2 q(max); the predicted effect for rho dominance is:

$$\frac{\frac{d\sigma}{dt}\text{ (meas)}}{\frac{d\sigma}{dt}\text{ (theory point charge)}} = \left|\text{EFF }(\pi)\right|^2 = \left(\frac{1}{1+\frac{q^2}{M_\rho^2}}\right)^2 ,$$

which is 0.77 at q(max) and 0.94 at one half q(max). One day's running will be 24 hours × 60 minutes × 15 pulses/minute = 21,600 pulses × 1 real event/pulse = 20,000 events. One real event can be obtained

with 10^6 π^+, so this gives a comfortable safety factor for background (could stand maybe 50 background trigger rate and still not sacrifice the real event rate) and a comfortable incident beam intensity of $\sim 4 \times 10^6$ particles of 3×10^6 p's and 1×10^6 π's. The high proton background cannot fake a real event in a direct manner, since $T_{e\max}$ for an incident proton is less than 6 GeV. If a good experiment consisted of 20 bins of 10^4 events each (1% statistics) or $\sim 2 \times 10^5$ events, then 10 days of data taking time would suffice for the $\pi^+ e^-$ experiment. Five days would allow a pe^- experiment as a check; additional time would allow a $K^+ e^-$ and $\mu^+ e^-$ experiment, although special enriched beams may be required for these latter experiments.

A good monitor for π^+'s is needed, one that has an absolute precision of better than 1%. An idea that might allow this precision might be collecting and integrating the Cerenkov light from the beam transport pipe from the production target to the experiment where a small amount of gas (e.g. 0.043 atm of H_2) is admitted to be above threshold for π's, but below K's and p's.

Equipment: The following list of items would be needed for the experiment and requested of NAL:

1 H-magnet 1 ft wide × 4 in. high × 3 m long 18 kG
1 C-magnet 1 ft wide × 8 in. high × 3 m long 18 kG
1 beam monitor of <1% precision
1 1/4 m × 2 cm diameter liquid hydrogen target
1 small computer with mag tape storage
1 DISC Cerenkov counter to measure the fraction of π^+ in the beam

REFERENCES

[1] J. Allen, G. Ekspong, P. Sallstrom, and K. Fisher, Nuovo Cimento 32, 1144 (64); D. Cassel, M. Barton, R. Crittenden, V. Fitch, and L. Leipuner (to be published).

[2] M. M. Block, I. Kenyon, J. Keren, K. Koethe, P. Malhotra, R. Walker, and H. Winzeler, Phys. Rev. (to be published).

[3] C. Mistretta, D. Imrie, J. A. Appel, R. Budnitz, L. Carroll, M. Goldstein, K. Hanson, and Richard Wilson, Phys. Rev. Letters 20, 1523 (68).

Table I. Techniques for Measuring the Pion Form Factor.

Experiment	Present Results	Method
1. π e elastic scattering [1]	$R_\pi < 3 \times 10^{-13}$ cm	direct experiment
2. $\pi^\pm \alpha$ elastic scattering [2]	$R_\pi < 1 \times 10^{-13}$ cm	interference effect
3. $e^- p \rightarrow e^- n \pi^+$ [3]	$R_\pi = 0.86 \pm 0.14 \times 10^{-13}$ cm	isolation of a single diagram

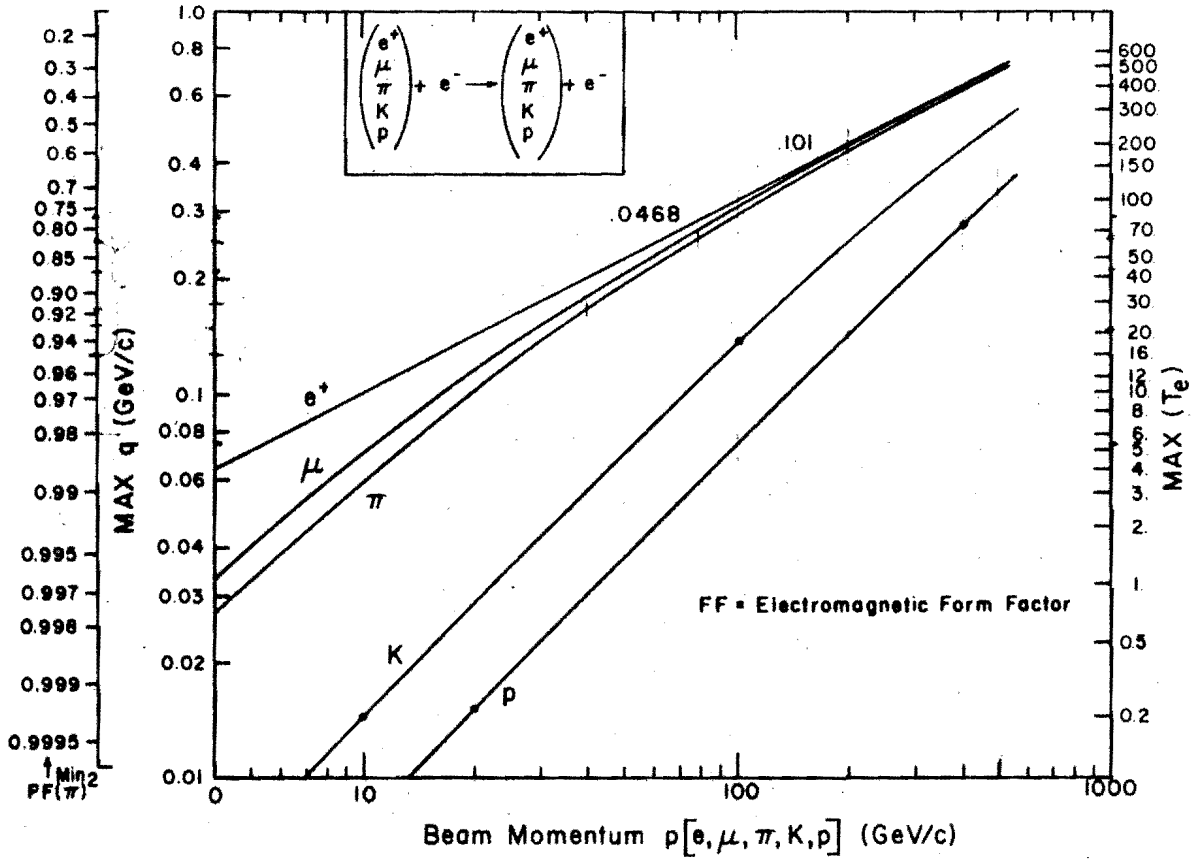

Fig. 1. Elastic scattering from electrons. The mass assumed in the expression for the form factor FF is that of the rho meson.

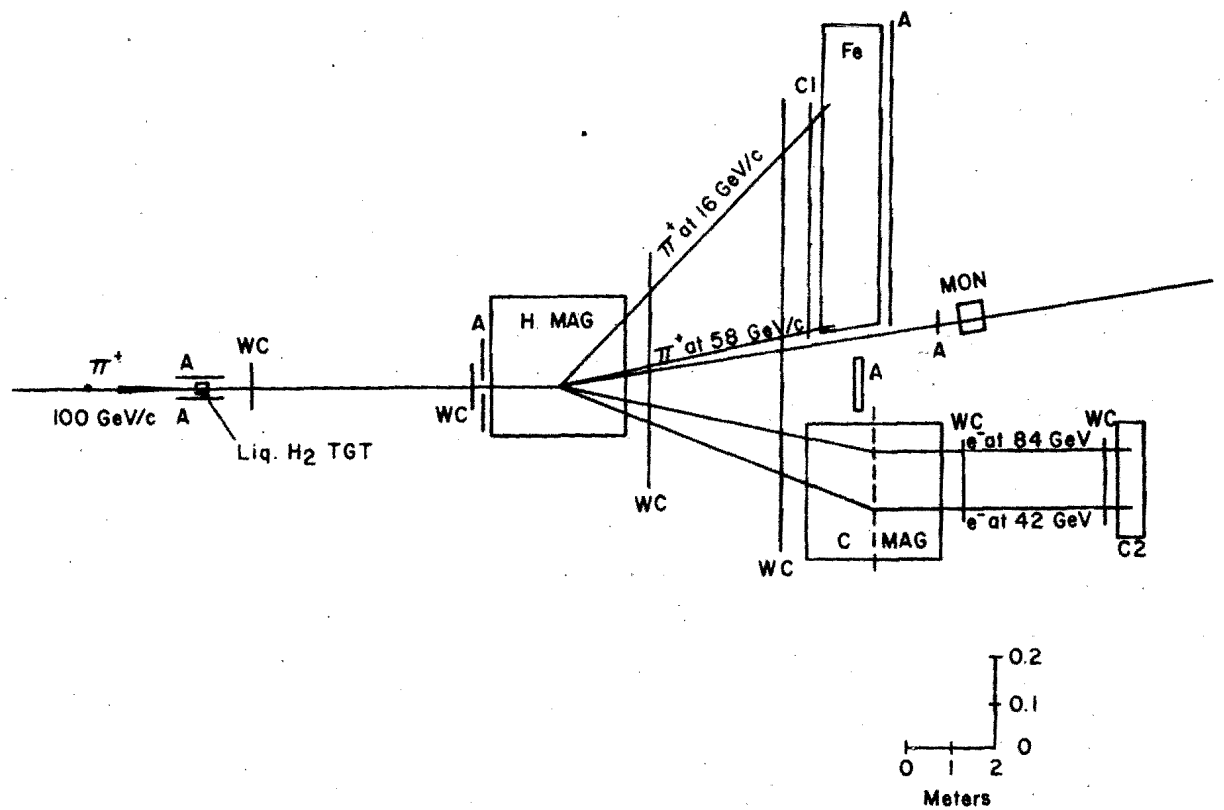

Fig. 2. Experimental layout for measuring scattering from electrons.